

Numerical Analysis of Characteristics of a Single U-tube Downhole Heat Exchanger in the Geothermal Reservoir

Xianzhi Song¹, Zehao Lyu¹, Gensheng Li¹, Mao Sheng¹, Jinxia Liu², Ruixia Li², Yu Shi¹

¹ State Key Laboratory of Petroleum Resources and Prospecting, China University of Petroleum, Beijing, Beijing 102249, China

² Sinopec Star Petroleum Co. Ltd, Beijing 100083, China

Keywords

Downhole heat exchanger; U-tube; flow field; heat transfer; numerical simulation

ABSTRACT

The heat extraction from the geothermal reservoir using a single U-tube has been widely applied in the last decades. Based on the geological data of Bazhou geothermal field, a 3D steady state numerical model, including the U-tube, wellbore and reservoir is established. The performance of the exchanger is studied through investigation on the influences of depth, porosity, permeability and heterogeneity of the formation. Simulation values are validated by results obtained from field tests. Results indicate that the overall velocity in the geothermal reservoir is relatively low compared with the flow in the wellbore mainly due to the high flow resistance. Under the conditions of this paper, the depth of the geothermal field, the reservoir porosity and the heterogeneity of the geothermal formation may hardly affect the performance of the U-tube. However, if it is possible, it is better to install the single U-tube in the homogeneous area of the reservoir, which may obtain better heat extraction effect.

1. Introduction

Geothermal energy has been considered as one of the most promising renewable and clean energy resources for the last several decades (Nasruddin et al., 2016; Lund et al., 2010). Downhole heat exchanger (DHE) is the most common form used to extract heat from the ground for space conditioning in residential and commercial buildings (Rees et al., 2015; Lee et al., 2008). DHE consists of a system of tubes or a U-tube located in a single wellbore, through which the working fluid is circulated to extract heat (**Fig. 1**). The vertical DHEs are usually constructed by inserting one or two high-density polyethylene U-tubes in vertical boreholes to serve as the ground loops (Zeng et al., 2003). Compared with other exploitation methods, such as Engineered Geothermal System, the U-tube only extracts heat from the geothermal reservoir instead of water

(Carotenuto *et al.*, 2001). This feature gives DHE some unique advantages, including low installation costs and least damage to the environment, etc.

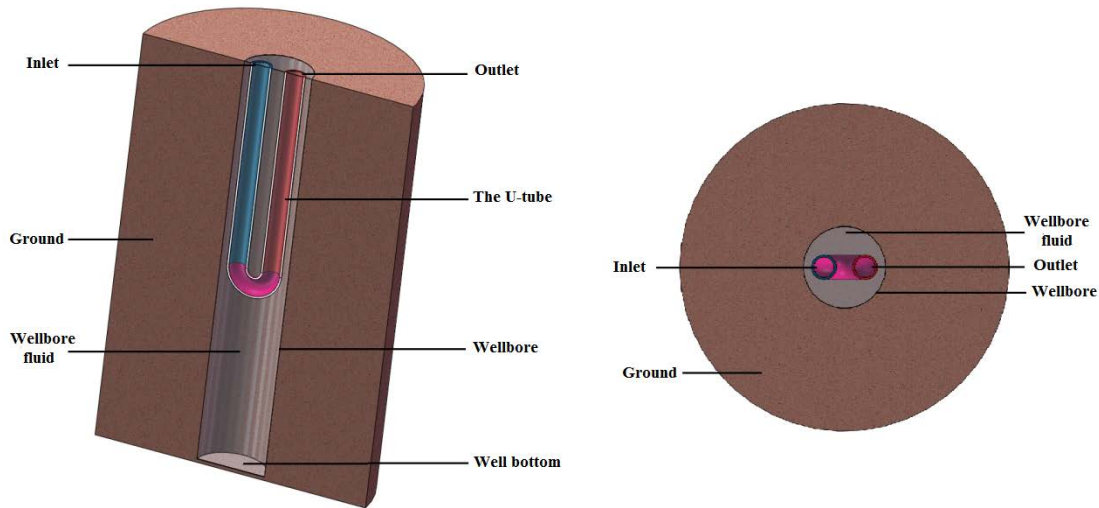


Figure 1: Schematic diagram of a single U-tube DHE geothermal system

A large number of investigations have been carried out on the heat extraction of DHE. In summary, those studies can be divided into two parts: the solid rock outside and the region inside the borehole. For the first part, Carotenuto *et al.* used a single domain numerical approach to describe the heat and fluid flow through saturated geothermal reservoir of DHE system (Carotenuto *et al.*, 2000). Besides, since the borehole depth is much larger than its diameter, this process is often formulated by 1D line-source (Ingersoll *et al.*, 2009) or cylindrical-source theory (Carslaw *et al.*, 1959; Kavanaugh *et al.*, 1985; Deerman *et al.*, 1991). Zeng *et al.* (2002) has presented a 2D model of the finite line-source to consider the axial heat flow in the ground for longer durations. For the second part, the main objective is to determine the entering and leaving temperatures of the circulating fluid in the exchanger. The temperature variation inside the borehole is usually slow and minor. Thus, the heat transfer in this region being approximated as a steady-state process has been proved to be suitable and described by a constant borehole thermal resistance, except for analysis dealing with dynamic responses within a few hours (Yavuzturk *et al.*, 1999). Eskilson *et al.* (1987) calculated the ground temperature around a single borehole using the finite-difference method and proposed a *g*-function to describe the performance of borehole and developed *g*-functions curves based on selected borehole field configurations. Li and Zheng (2009) developed a 3D unstructured finite-volume model for vertical ground heat exchanger and used Delaunay triangulation to mesh the computational domain. The surrounding soil was divided into several layers to evaluate the effect of fluid temperature with depth on the thermal process. Besides, a transient finite-volume model was developed by Kaltreider *et al.* (2015) specifically for modeling thermo-active foundation. Rees and He (2013) used a multi-block mesh to establish a 3D model to investigate the effects of fluid transport and diffusion on the fluid flow physical phenomenon. Lyu *et al.* (2017) proposed a steady-state numerical model, which coupled working fluid in DHE with geothermal fluid inside wellbore, to investigate the influences of key parameters on heat extraction performance of a U-tube DHE.

In view of the complexity of the heat transfer in DHE, Computational Fluid Dynamics (CFD) has been widely used in the previous study listed above (Bhutta *et al.*, 2012). Xie *et al.* (2009)

evaluated the Nu and friction factor for three types of fin and tube heat exchangers. Study was conducted to observe the difference between laminar and turbulent heat transfer for larger diameter of tubes. Starace and Congedo *et al.* (2005) evaluated horizontal GSHPs based on experiments and simulations. The main parameters affecting the performance of horizontal ground heat exchangers were investigated by the CFD code Fluent (Congedo *et al.*, 2012). Gustafsson *et al.* (2010) studied the performance of a U-pipe in a groundwater-filled heat exchanger in Scandinavia using a 3D steady state CFD model. The results show that the induced natural convection significantly decreases the thermal resistance inside the borehole. Habchi *et al.* (2010) observed heat transfer parameters and the turbulent mixing in the multi-functional heat exchanger under three different configurations. The Laser Doppler analysis and the CFD approach were used to determine the consequences of the vorticity produced by the trapezoidal tabs.

However, to the best of our knowledge, there is no comprehensive study on the coupled flow field of working fluid in a single U-tube DHE, geothermal fluid inside the wellbore and flow in the reservoir. In this paper, Bazhou geothermal field in China is taken as a case to be studied. First, a 3D steady-state numerical model is established to combine the entire flow field of both wellbore and reservoir. Second, the flow field is analyzed comprehensively considering characteristics of the working fluid emphatically. Simulation values are validated by comparing with results obtained from field tests. Finally, influences of four important geological parameters, including depth, porosity, permeability and heterogeneity of the formation, on the performance of the DHE are investigated. Results in this paper can provide guidance for the field application of vertical DHE.

2. Model development

2.1 Physical model

The simulation model is based on a small-scale field case. For the heat extraction of a single U-tube, the entire simulation model consists of three parts: the U-tube, borehole and ambient geothermal reservoir. Consequently, a 3D model is established as shown in **Fig. 2**. In this paper, the geological parameters of Bazhou geothermal field in China are taken as an example for simulation. The working fluid is water, which is injected from the inlet of the U-tube to exchange heat with the borehole fluid and backs upward from the outlet. When the borehole fluid temperature varies because of the heat transfer, changes in the density occur. Dense fluid will start to sink and less dense fluid to rise, resulting in the natural convection within the entire downhole wellbore, which leads to a better heat transfer through the borehole fluid (Gustafsson *et al.*, 2010).

The geothermal energy in Bazhou geothermal field, mostly locates in shallow formations. Therefore, in this paper, the entire heat transfer process mainly occurs under the hydrostatic pressure of 2 MPa when it is 200 m under the ground. The U-tube heat exchanger is lowered to the downhole position above the geothermal reservoir. The hydrostatic height of fluid in the wellbore maintained by the reservoir pressure is assumed to be larger than 3 m, which can satisfy the heat extraction simulation in this paper. The borehole fluid is water and the borehole length is 6 m. The borehole diameter is set as 0.35 m. Besides, the geothermal reservoir or ground is a cylinder with a diameter of 3 m and a height of 2.8 m. According to Allis *et al.* (1980), the U-tube inlet and outlet diameter is set as 0.0875 m. The injected circulating water temperature is set

as 298 K. The borehole fluid temperature is 353 K. The reservoir porosity is 0.35 and the permeability is uniformly distributed in three spatial directions with a value of 1.0 Dc. Other related parameters are illustrated in **Table 1**.

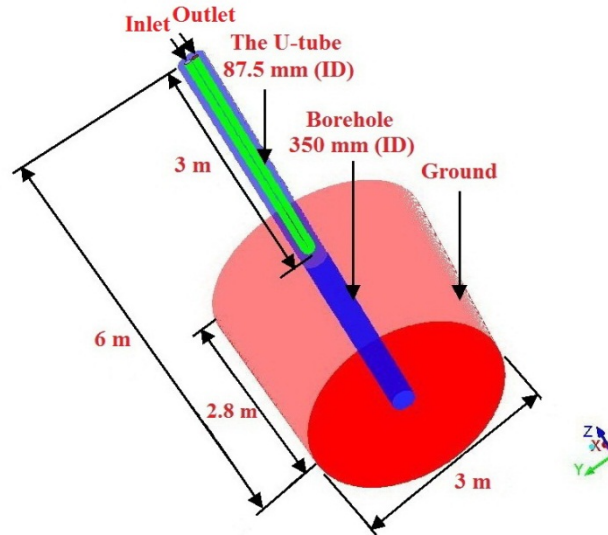


Figure 2: The physical model of a single U-tube in the geothermal reservoir

Table 1 Mathematical parameters of the model

The entire U-tube length (m)	Borehole length (m)	Borehole diameter (m)	Distance between the U-tube inlet and outlet (m)	The U-tube inlet and outlet diameter (m)
6.16	6	0.35	0.1	0.0875

The entire numerical solution process is based on the CFD code of Fluent. In order to simulate the turbulent flow in the U-tube, the time-averaged steady state Navier-Stokes equations as well as the conservation of energy are solved. The standard $k-\varepsilon$ model (Takemitsu et al., 1990) is adopted and the pressure-velocity field is coupled by SIMPLE algorithm. The heat transfer between the U-tube and borehole fluid mainly depends on the natural convection caused by gravity (Gustafsson et al., 2010). Therefore, gravity is considered in the Z direction.

2.2 Thermo-physical properties of water

In the convection heat transfer process of the U-tube, as described by Lyu et al. (2017), the water density and the specific heat capacity are the two most important factors to affect the heat transfer process, while the thermal conductivity and the viscosity are assumed to be constant. In this paper, the U-tube DHE works under a constant underground pressure. To simulate this process specifically, changes of water properties with temperature are determined using the least square and fitting methods (Wagner et al., 2002).

The water density decreases as the increase of temperature in the temperature range of 275 K ~ 420 K (**Fig. 3**) and the relationship is shown in Eq. (1). The specific heat capacity of water

decreases first, and then goes up with the increment of temperature (**Fig. 4**). The correlation is displayed in Eq. (2). Besides, the water viscosity is 0.001003 kg/m/s and thermal conductivity is 0.6 W/m/K.

$$\rho = -0.0029T^2 + 1.418T + 829.99 \quad (1)$$

$$C_p = 0.011T^2 - 6.9573T + 5278.3 \quad (2)$$

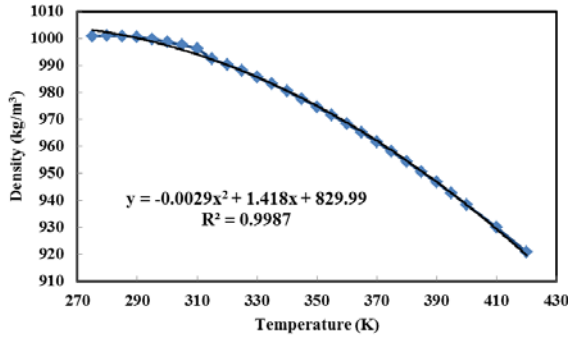


Figure 3: Water density as a function of temperature at 200 m

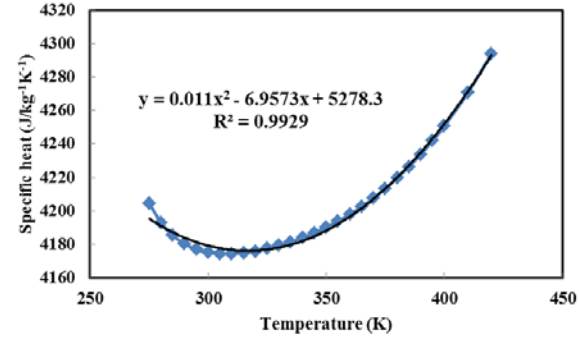


Figure 4: Water specific heat capacity as a function of temperature at 200 m

2.3 Heat transfer coefficient

Several factors can have an influence on the heat transfer between the U-tube and geothermal reservoir, including the cause of the flow, fluid phase, flow state, geometrical factors of the heat transfer surface and fluid properties. In this paper, the water in the U-tube is pumped to circulate, which is the forced convection heat transfer. The heat transfer with the downhole geothermal fluid belongs to the natural convection process. There is no phase change in the entire heat transfer process. The final values of convection heat transfer coefficient were specifically listed by Lyu *et al.* (2017), here we only concisely illustrate the procedures of calculation.

The convection heat transfer coefficient represents the intensity of the heat transfer process. It can be determined by Eq. (3):

$$h = \frac{Nu \cdot \lambda_f}{d_0} \quad (3)$$

Where Nu is the Nusselt number. λ_f is fluid thermal conductivity, $W/(m \cdot K)$. d_0 is the internal diameter of the U-tube.

There are mainly two equations (Dittus-Boelter and Gnielinski) to calculate the Nusselt number of fluid. In the Dittus-Boelter model (Heiss *et al.*, 1951), the Nusselt number is calculated by Eq. (4):

$$Nu = 0.023 Re_f^{0.8} Pr_f^n \quad (4)$$

Where $n=0.4$. Re_f is the Reynolds number. Pr_f is the Prandtl number. The equation is validated via experiments when $Re_f = 10^4 \sim 1.2 \times 10^5$, $Pr_f = 0.7 \sim 20$, $l/d_0 \geq 60$. l is the length of the U-tube. However, the temperature difference between the fluid and environment is limited to $20 \sim 30$ K. In this paper, the temperature difference is usually about 50 K. Thus, it is not suitable to use this model to calculate the convection heat transfer coefficient.

In the Gnielinski model [32], the Nusselt number is calculated by Eq. (5):

$$Nu = \frac{(f/8)(Re_f - 1000)Pr_f}{1 + 12.7\sqrt{f/8}(Pr_f^{2/3} - 1)} \left[1 + \left(\frac{d_0}{l}\right)^{2/3}\right] c_t \quad (5)$$

Where f is the Darcy drag coefficient of internal turbulent flow. For the fluid, c_t is nearly equal to 1. In this paper, the length of the U-tube l is much larger than the internal diameter d_0 .

Therefore, the part in Eq. (5) $1 + \left(\frac{d_0}{l}\right)^{2/3} \approx 1$.

Then, the Eq. (5) is simplified to Eq. (6) as shown below:

$$Nu = \frac{(f/8)(Re_f - 1000)Pr_f}{1 + 12.7\sqrt{f/8}(Pr_f^{2/3} - 1)} \quad (6)$$

The Darcy drag coefficient f can be calculated by Filonenko equation (Filonenko et al., 1990):

$$f = (1.82 \lg Re_f - 1.64)^{-2} \quad (7)$$

This model is validated when $Re_f = 2300 \sim 10^6$, $Pr_f = 0.6 \sim 10^5$.

Because each temperature corresponds to each convection heat transfer coefficient, the average temperature of inlet circulating water and borehole water is applied as the reference temperature to determine the convection heat transfer coefficient.

2.4 Heat extraction rate

Heat extraction rate represents the portion of energy that can be used through a U-tube DHE in geothermal wells. The Eq. (8) is applied to calculate the heat extracted from the downhole U-tube.

$$Q = C_{p2}mT_2 - C_{p1}mT_1 \quad (8)$$

Where Q is the heat extraction rate, KW . C_{p1} is the specific heat capacity of the inlet fluid, $J/(kg \cdot K)$. C_{p2} is the specific heat capacity of the outlet fluid, $J/(kg \cdot K)$. m is the mass flow rate, kg/s .

2.5 Mesh independency and boundary conditions

To guarantee the simulation results are mesh-independent, meshes with different grid numbers are computed and illustrated by **Fig. 5**. The average outlet temperature is used as the indicator of mesh sufficiency. **Fig. 5** shows that after the grid number is larger than 1.5×10^6 (red point), the average outlet temperature stays almost constant. In addition, in view of computational precision and complexity, it is acceptable to choose the red point as the final mesh. Therefore, the numerical mesh consists of a total of 1735094 cells of hexahedron and wedge-shaped volume elements in the U-tube, borehole and geothermal reservoir.

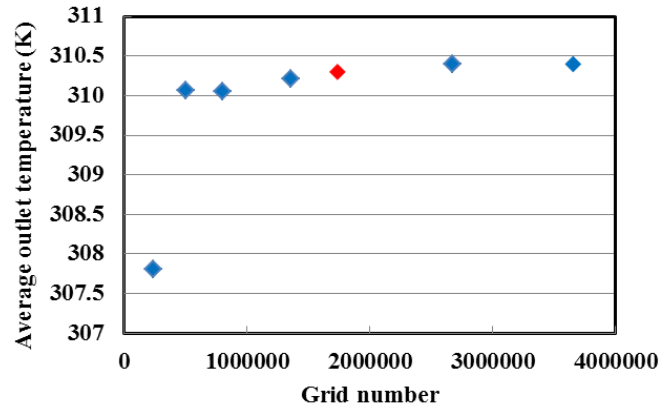


Figure 5: Average outlet temperature at different grid numbers

According to conditions for the heat transfer between the U-tube and the geothermal fluid (**Fig. 2**), the circulation water inlet is set as the mass-flow-inlet boundary condition. The outer boundary of porous geothermal reservoir (ground) is set as a constant temperature and the bottom and top boundaries are treated as adiabatic surfaces (Gustafsson *et al.*, 2010). The operating pressure varies with the depth of geothermal formation. In addition, the natural convection heat transfer coefficient between the U-tube and the borehole fluid is updated with each mass flow rate of the circulating water.

3. Results and discussion

3.1 Underground flow field

This paper mainly focuses on the investigation of underground flow field. **Fig. 6** shows the flow field in the geothermal reservoir from the front perspective. It can be observed that the overall velocity is very low mainly because of two reasons. The first is that the drive force is just the heat convection as discussed above. The second reason is that compared with the wellbore, the flow resistance is very high due to the packed particles in the reservoir. In the selected section, the maximum velocity is only 2.42×10^{-11} m/s, which lies in the region close to the central wellbore. Besides, **Fig. 6** only shows the flow direction of fluid in the reservoir within a certain velocity range. It can be inferred that the velocity in the wellbore can several magnitudes higher than that in the reservoir.

In addition, there are two circulations existing around the wellbore. In this paper, the geothermal fluid at the left side is anti-clockwise, while the right one is clockwise. This is because the U-

tube simulated in this model is located above the geothermal reservoir. The temperature of the wellbore fluid around the U-tube is lowered due to the heat transfer, resulting in the increase of density. With the effect of gravity, the upper heavier wellbore fluid sinks to the lower part of the wellbore, which drives the geothermal fluid to begin circulating in the reservoir from the upper connection between the wellbore the ground. Then the geothermal fluid returns to the wellbore space to participate in the complicated flow in the wellbore.

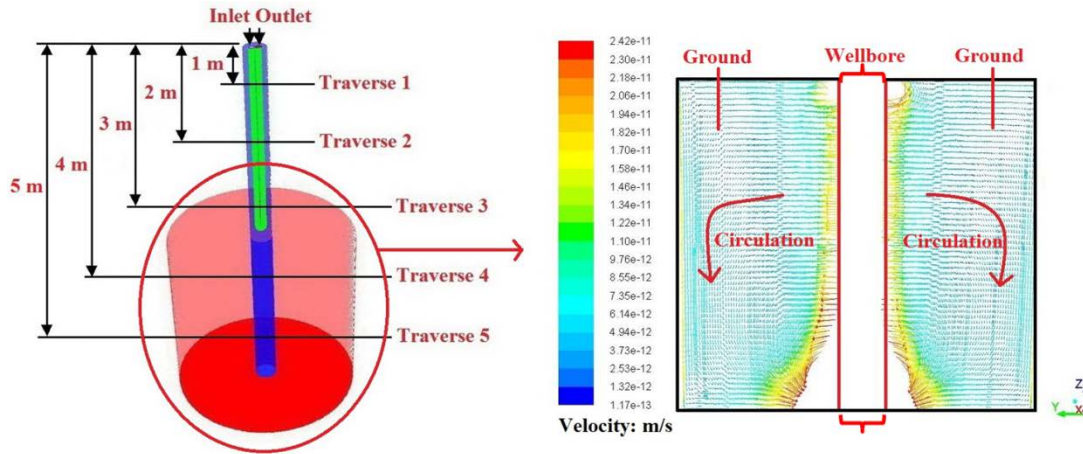


Figure 6: The flow field in the geothermal reservoir

To analyze the characteristics of the flow pattern more specifically, four traverses are chosen distributed along the borehole uniformly (**Fig. 6**). **Traverse 1 to 3** is above the reservoir, while **Traverse 4 and 5** are distributed within the reservoir. **Fig. 7** shows the flow state at **Traverse 4** and **5**. It can be observed that they are similar to each other. The fluid flows out from the wellbore at a relatively higher velocity in both radial and gravitational directions. Then the velocity becomes lower during the flow process until the fluid encounters the outer boundary of the reservoir. The maximum velocity can be approximately 2×10^{-11} m/s, which is slightly lower than the vertical plane (**Fig. 7**).

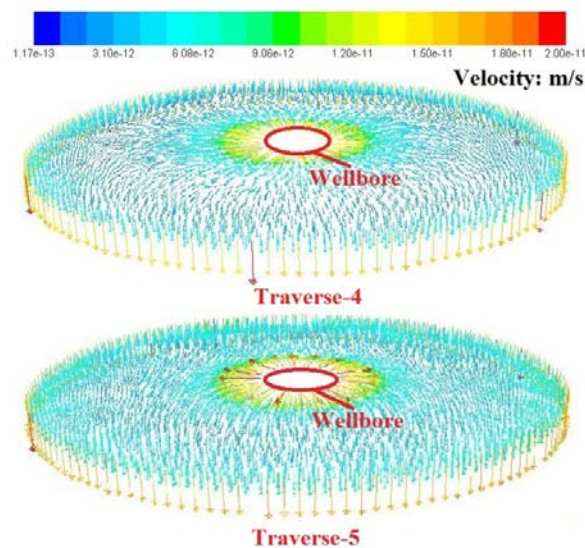


Figure 7: Vectors of velocity at Traverse 4 and 5

To compare the overall flow state in the whole heat extraction system, **Fig. 8** shows the average velocities of various traverses at different injection fluid mass flow rates. The average velocities in the wellbore go up as the increase of mass flow rate. However, the average velocities in the geothermal reservoir keep almost the same. Besides, the velocities of **Traverse 1** and **2** are nearly the same. **Traverse 3** is slightly higher. The order of magnitude is roughly 10^{-2} m/s. Nevertheless, the order of magnitude of velocities in the reservoir is approximately 10^{-10} m/s. Besides the reason of high flow resistance as discussed above, another probable reason is that the calculated average velocity in the wellbore part contains the flow in the U-tube, which is relatively high. However, one point that needs to be made is that the velocity becomes higher due to the sharp U-shape turn (**Traverse 3**). Additionally, the mass flow rate can hardly affect the flow in the reservoir.

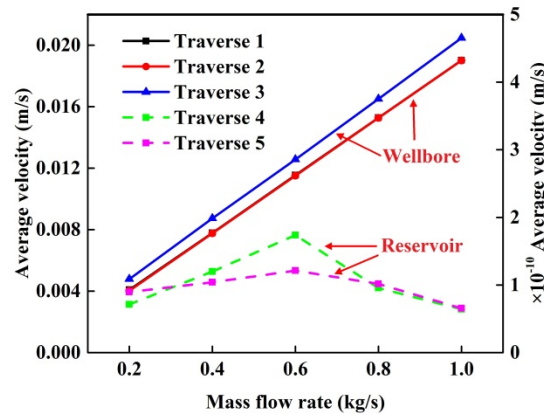


Figure 8: Average velocities of various traverses at different water mass flow rates

Fig. 9 shows the temperature distributions of fluid flow along the entire U-tube at different mass flow rates. It is clear that the injected low temperature water is heated up from 293 K to approximately 310 K during the flow process. As the mass flow rate rises, the average temperature in the outlet (right) side of the U-tube becomes lower. The relatively low temperature region (below 300 K, deep blue area) becomes larger.

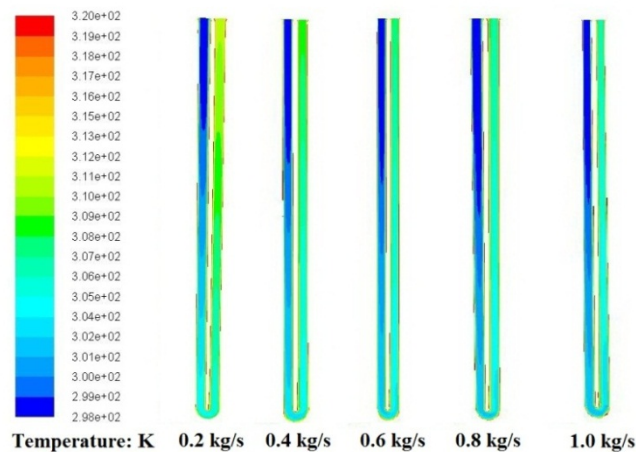


Figure 9: Temperature contours of the entire U-tube at different water mass flow rates

3.2 Model validation

To validate the simulation results in this paper, the field test results obtained by Carotenuto *et al.* (1999) are adopted. The field tests were performed in the Campi Flegrei geothermal field, in the Lacco Ameno area of the island of Ischia. The aquifer with geothermal fluid temperature of 73.3°C was found at a depth of approximately 10 m from ground level. The downhole effective heat transfer vertical length is 6.16 m. The effective contact vertical thickness between the wellbore and geothermal reservoir is 3 m. The 500 mm diameter well was lined with steel piping with an outside diameter of 380 mm. Although there are two phases in the experimental geothermal convector, it is mainly in the liquid state in the downhole U-tube section, which approximates the situation in this paper. Since the experiments were carried out at the depth of 10 m under the ground, thermo-physical properties of water have to be calculated by Eq. (9) and (10). **Fig. 10** and **Fig. 11** show the water density and specific heat capacity as a function of temperature at the depth of 10 m. Through least square method, the relationships between the water density, specific heat capacity and temperature can be obtained as follows:

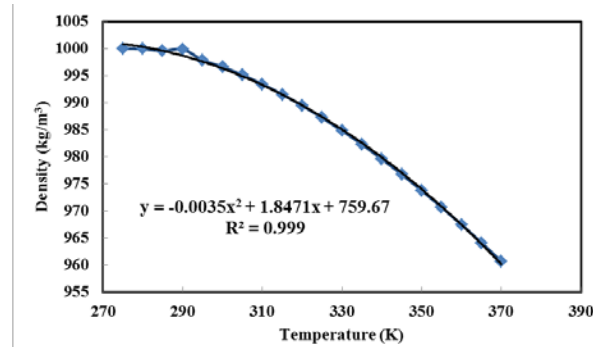


Figure 10: Water density as a function of temperature at 10 m

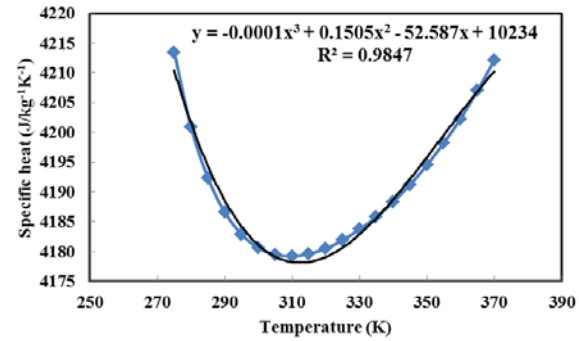


Figure 11: Water specific heat capacity as a function of temperature at 10 m

$$\rho = -0.0035T^2 + 1.8471T + 759.67 \quad (9)$$

$$C_p = -0.0001T^3 + 0.1505T^2 - 52.587T + 10234 \quad (10)$$

Fig. 12 shows the comparison of simulation and field test results at different mass flow rates. Compared with the actual field test results, the modeled values are all within reasonable ranges. In some cases, the simulation values are slightly lower than the experimental results. Besides computational errors, this is also because the entire length of the U-tube in the model is slightly shorter than that in the field test and the effective formation thickness is small. Therefore, it can be concluded that the simulation results are greatly reliable.

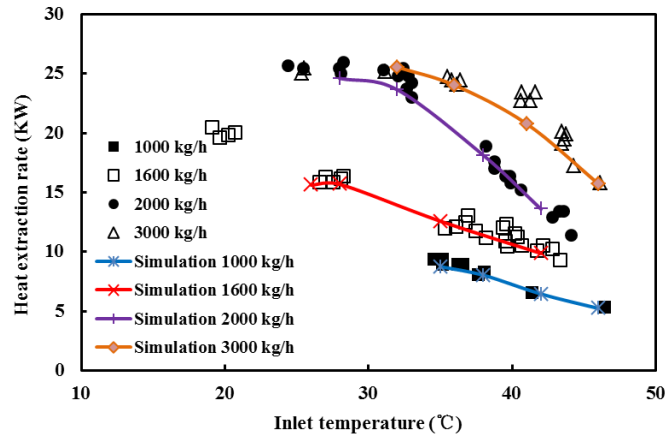


Figure 12: Comparison of simulation values and field test results

3.3 Parameter analysis

3.3.1. Depth

In addition to the Bazhou geothermal field analyzed in this paper, there are many other fields around the globe, which has a large range of effective formation thickness at the depths of 100 m, 200 m, 300 m, etc. Some may have the same geothermal temperature. In this case, the thermo-physical properties of the water may play an important role in the performance of heat extraction. As described above, the density and specific heat capacity of water are calculated at the depth of 100 m as shown in **Fig. 13** and **Fig. 14**.

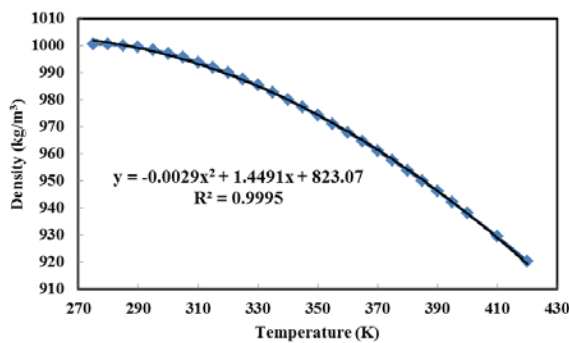


Figure 13: Water density as a function of temperature at 100 m

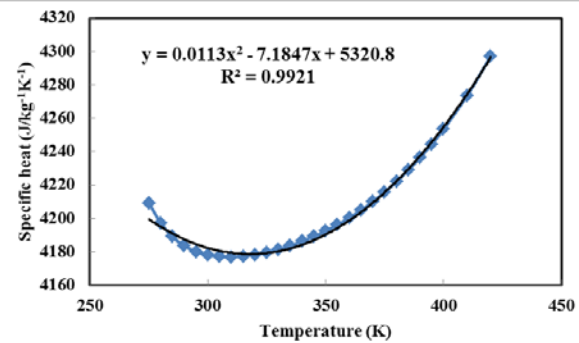


Figure 14: Water specific heat capacity as a function of temperature at 100 m

Fig. 21 shows the performance of a single U-tube DHE at different depths. The initial water inlet temperature is 298 K and the geothermal fluid temperature is 353 K. When the water mass flow rate is 0.2 kg/s, the circulating water temperature can be heated up by approximately 12 K. The outlet temperature becomes lower as the flow rate increases. The outlet temperature is less and less sensitive to the variation of flow rate. The heat extraction rate shows almost linear relationship with the flow rate. When the depth increases from 100 m to 300 m, the outlet temperature has an appreciable rise only at low mass flow rates. However, heat extraction rates at different depths are almost the same. Therefore, under the condition of the same temperature difference between the circulating water in the U-tube and the borehole fluid, the depth of the geothermal field has little influence on the outlet temperature and heat extraction rate.

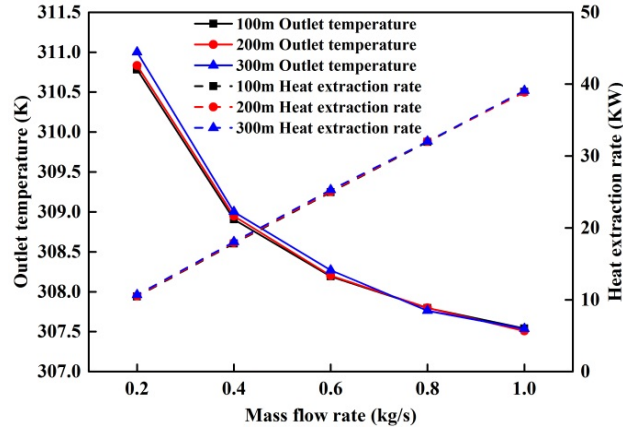


Figure 15: Performance of the U-tube at different depths

3.3.2. Porosity

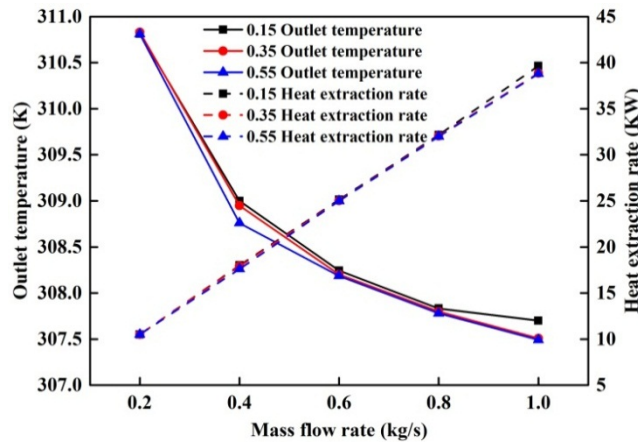


Figure 16: Performance of the U-tube at different reservoir porosities

Different geothermal formations can have various porosities. Besides, for the same geothermal formation, the porosity can be distributed non-uniformly. In this section, the simulated reservoir is assumed to be homogeneous and have the same porosity. **Fig. 16** shows the performance of the U-tube with reservoir porosity changing from 0.15 to 0.55. It can be observed that at each mass flow rate, the final outlet temperatures of different porosities are similar. To be more precise, the outlet temperature decreases as the increase of porosity. As for the heat extraction rate, there is almost no difference between different porosities at each mass flow rate. Therefore, it can be concluded that the reservoir porosity may hardly affect the performance of the U-tube.

3.3.3. Permeability

To simulate the fluid flow in the formation, the porous media model is applied to represent the flow resistance in the geothermal reservoir. The momentum equation can be simplified into Eq. (11) by considering the pressure difference resulting from the source term.

$$\nabla p = -\left(\frac{\mu}{\alpha} v + C_2 \frac{1}{2} \rho v^2\right) \Delta n \quad (11)$$

Where ∇p is the pressure difference, Pa. μ is the fluid viscosity, kg/m/s. D_p is the average diameter of particles, m. ε is the porosity. $1/\alpha$ is the coefficient of viscous impedance. C_2 the coefficient of internal impedance. ρ is the density, kg/m³. v is the reservoir flow velocity, m/s. Δn is the thickness of the porous media.

Then the relationship between the pressure difference ∇p and the reservoir flow velocity v has to be determined. Eq. (12) is derived by combining the Darcy's law (Eq. (13)) with the integral of radial fluid flow.

$$\Delta p = r \frac{\mu}{k} \ln\left(\frac{r_e}{r_w}\right) v_r \quad (12)$$

$$\nabla p = -\frac{\mu}{\alpha} v \quad (13)$$

Where k is the reservoir permeability, m². r_e is the radius of the entire reservoir, m. r_w is the wellbore radius, m. v_r is the fluid flow velocity at the radial distance of r , m/s.

By comparing Eq. (12) and Eq. (11), the coefficient of viscous impedance $1/\alpha$ can be obtained as displayed in Eq. (14).

$$\frac{1}{\alpha} = -r \frac{\mu}{k \Delta n} \ln\left(\frac{r_e}{r_w}\right) \quad (14)$$

The relationship between the reservoir permeability and viscous impedance is established in Eq. (14). To represent the overall flow state in the simulated reservoir, the average radius is chosen for the calculation. **Fig. 17** shows that the coefficient of viscous impedance decreases as the increase of the reservoir permeability.

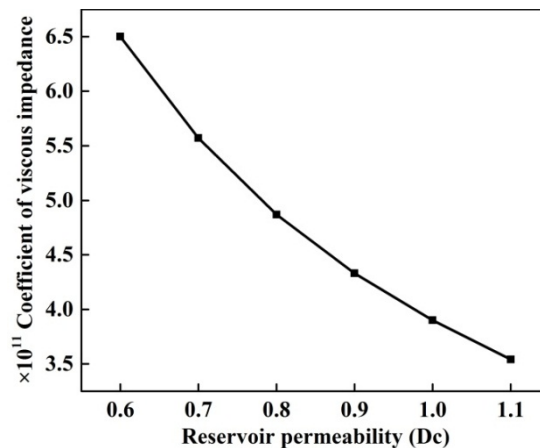


Figure 17: Relationship between the coefficient of viscous impedance and reservoir permeability

In this section, the reservoir formation is assumed to be homogeneous, which means that the permeability is the same in all directions. The heterogeneity of the formation will be discussed in the next section. **Fig. 18** shows the outlet temperature and heat extraction rate under different

conditions. It can be observed that the outlet temperature and extraction rate keeps nearly the same at the mass flow rate of 0.2 kg/s. However, at higher mass rates, such as 0.4 kg/s, 0.6 kg/s and 0.8 kg/s, the outlet temperature slightly increases. This may be because the convective heat transfer between the fluid in the U-tube and the geothermal fluid becomes more drastic, when the mass flow rate rises. In formations with high permeability, the circulation in the wellbore and reservoir may become more rapid, which results in the slightly better performance. Nevertheless, the overall influence of the reservoir permeability on the U-tube performance is minor. Under the conditions of this paper, the heat extraction rates are nearly the same in different geothermal formations.

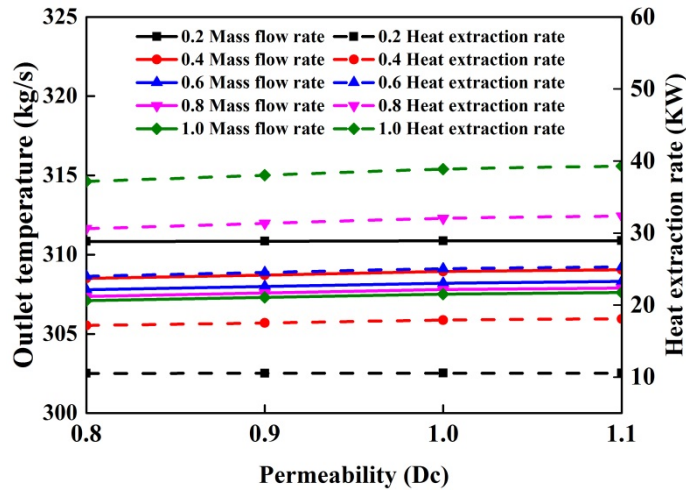


Figure 18: Performance of the U-tube at different reservoir permeability

3.3.4. Heterogeneity of the formation

In the real geothermal field, the reservoir is usually heterogeneous. The permeability in each direction can be different from each other. If the heat extraction method using a single U-tube is applied as shown in **Fig. 19**, the low temperature water is pumped from one side and the heated water backs upward from the opposite side. Considering the case of different permeability in various directions and the way of low temperature fluid injection, this is similar to the problem that drilling horizontal wells for hydraulic fracturing in formations with different in-situ stresses. Therefore, to investigate the effect of heterogeneity and position of the U-tube, the permeability of the formation is changed in each direction (x , y , z), while the other two directions is kept the same.

In **Fig. 20**, the x -direction permeability is changed from 0.8 Dc to 1.1 Dc, while the permeability in y and z directions keeps at 1.0 Dc. As shown in **Fig. 19**, the x -direction is perpendicular to the dash line connecting the inlet and outlet. The simulation results show that the effect of x -direction permeability on the U-tube performance at different mass flow rates is minor. To be more precise, as labeled in points of heat extraction rate at 0.2 kg/s and 0.6 kg/s, the value increases slightly and peaks at the permeability of 1.0 Dc. However, when the x -direction permeability changes to be 1.0 Dc, the geothermal reservoir actually becomes homogeneous. This result indicates that the single U-tube may work better in the uniform reservoir.

To analyze whether the performance of the U-tube is related to the permeability direction, in **Fig. 21**, the y-direction permeability is changed from 0.8 Dc to 1.1 Dc, while the permeability in x and z directions is 1.0 Dc. The y-direction is parallel to the straight line connecting the inlet and outlet. However, similar results are obtained compared with **Fig. 20**. The outlet temperature and heat extraction rate also peaks at the permeability of 1.0 Dc. This result indicates that the installed position of the U-tube can hardly affect the performance.

Similarly, the z-direction permeability is changed from 0.8 Dc to 1.1 Dc. As shown in **Fig. 22**, the outlet temperature and heat extraction rate exhibit similar characteristics compared with **Fig. 20** and **Fig. 21**. Therefore, in summary, the heterogeneity of the geothermal formation may have little influence on the performance of the U-tube.

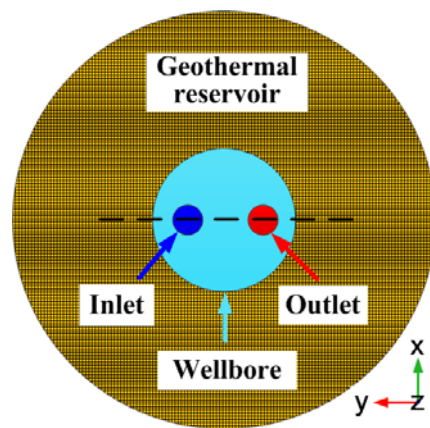


Figure 19: Schematic of a single U-tube in the geothermal reservoir

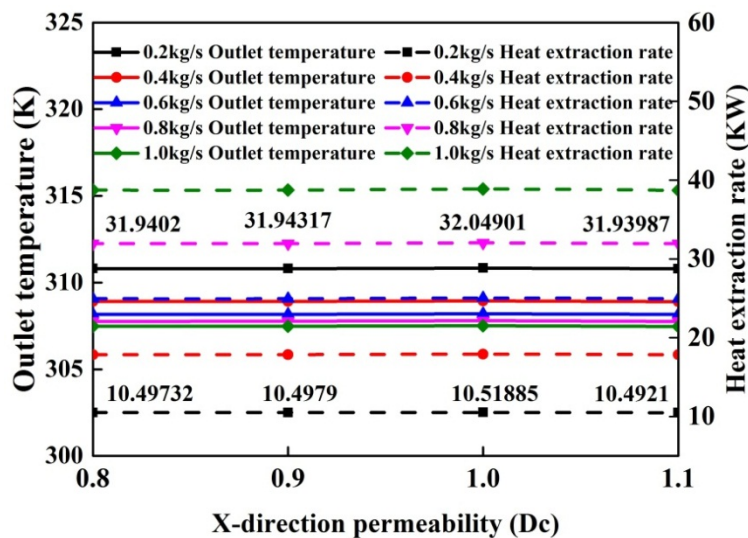


Figure 20: Performance of the U-tube at different x-direction permeability

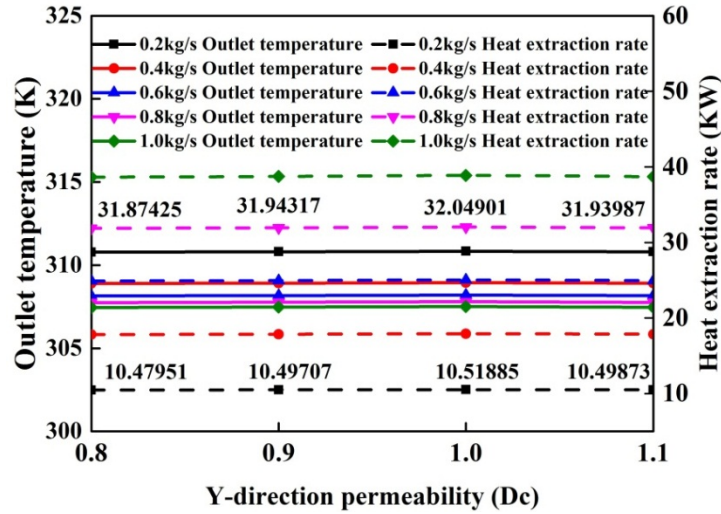


Figure 21: Performance of the U-tube at different y-direction permeability

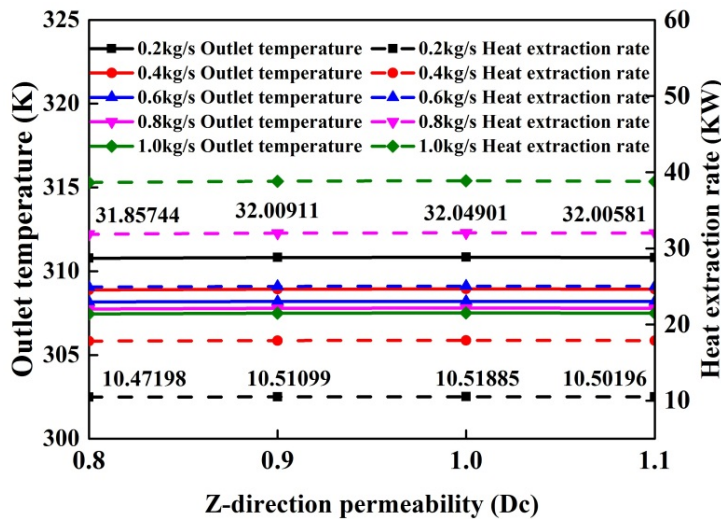


Figure 22: Performance of the U-tube at different z-direction permeability

4. Conclusions

In this paper, the performance of a single U-tube DHE in Bazhou geothermal field is analyzed comprehensively, from aspects of depth, porosity, permeability and heterogeneity. Simulation values are validated by results obtained from field tests. Based on the results of this study, the following conclusions are drawn:

- (1) The overall velocity in the geothermal reservoir is very low mainly because of two reasons. The first is that the drive force is just the heat convection. The second reason is that compared with the wellbore, the flow resistance is very high. The order of magnitude of velocities in the reservoir is approximately 10^{-10} m/s. Nevertheless, the

order of magnitude in the wellbore is roughly 10^{-2} m/s. In addition, there are two circulations existing around the wellbore. Besides, the mass flow rate can hardly affect the flow in the reservoir.

- (2) Under the condition of the same temperature difference between the circulating water in the U-tube and the borehole fluid, the depth of the geothermal field has little influence on the outlet temperature and heat extraction rate.
- (3) The outlet temperature decreases slightly as the increase of porosity. As for the heat extraction rate, there is almost no difference between different porosities at each mass flow rate. Therefore, it can be concluded that the reservoir porosity may hardly affect the performance of the U-tube.
- (4) Under the conditions of this paper, the heat extraction rates are nearly the same in different geothermal formations with isotropic permeability. Heterogeneity of the formation and the installed position of the U-tube are analyzed. Results indicate that the single U-tube may work better in the homogeneous reservoir. The installed position of the U-tube can hardly affect the performance. Besides, the heterogeneity of the geothermal formation may have little influence on the performance of the U-tube.

Acknowledgments

The authors would like to acknowledge the Newton Fund – China – UK Joint Research: GeoSmart Wells: smart technologies for optimal drilling, completion, design and management of geothermal wells (2016YFE0124600), Program of Introducing Talents of Discipline to Chinese Universities (111 Plan) (B17045) and National Natural Science Foundation of China (51504272, U1562212, 51521063). Besides, support from Special Fund of Ministry of Education for Authors of Outstanding Doctoral Dissertations (201352) and China National Petroleum Corporation Innovation Fund (2015D-5006-0308) and New Technique and Method Fund (2016A-3902) are appreciated.

REFERENCES

- Allis R G, James R. A natural convection promoter for geothermal wells[J]. Geothermal Resources Council Transaction 1980,4: 409-412.
- Bernier M A. Ground-coupled heat pump system simulation[J]. Ashrae Transactions, 2001, 107:605-616.
- Bhutta M M A, Hayat N, Bashir M H, et al. CFD applications in various heat exchangers design: A review[J]. Applied Thermal Engineering, 2012, 32(1):1-12.
- Carotenuto A, Casarosa C, Vanoli L. Optimizing the position of the tube casing slotted section for geothermal wells with a downhole heat exchanger[J]. Geothermics. 2001, 30:133-57.
- Carotenuto A, Casarosa C. A lumped parameter model of the operating limits of one-well geothermal plant with down hole heat exchangers[J]. International Journal of Heat & Mass Transfer. 2000, 43:2931-48.

- Carslaw H S, Jaeger J C, Feshbach H. Conduction of Heat in Solids[M]. Clarendon Press, 1959.
- Carotenuto A, Casarosa C, Martorano L. The geothermal convector: experimental and numerical results[J]. Applied Thermal Engineering, 1999, 19(19):349-374.
- Congedo P M, Colangelo G, Starace G. CFD simulations of horizontal ground heat exchangers: A comparison among different configurations[J]. Applied Thermal Engineering, 2012, s 33–34(1):24-32.
- Deerman J D. Simulation of Vertical U-tube Ground-coupled Heat Pump Systems using the Cylindrical Heat Source Solution[J]. Ashrae Transactions, 1991, 97(1):287-295.
- Eskilson P. Thermal analysis of heat extraction boreholes[J]. 1987.
- F.D. Incropera, D.P. DeWitt, Fundamentals of Heat and Mass Transfer, John Wiley and Sons, New York, 1990.
- Gustafsson A M, Westerlund L, Hellström G. CFD-modelling of natural convection in a groundwater-filled borehole heat exchanger[J]. Applied Thermal Engineering, 2010, 30(6–7):683-691.
- Gnielinski, V. new equations for heat and mass-transfer in turbulent pipe and channel flow[J]. International Chemical Engineering, 1976, 16(2):359-368.
- Habchi C, Lemenand T, Valle D D, et al. Turbulent mixing and residence time distribution in novel multifunctional heat exchangers–reactors[J]. Chemical Engineering & Processing Process Intensification, 2010, 49(10):1066-1075.
- Heiss J F, Coull J. Nomograph of Dittus-Boelter Equation for Heating and Cooling Liquids[J]. Industrial & Engineering Chemistry, 1951, 43(5):1226-1229.
- Ingersoll L R, Zobel O J, Ingersoll A C. Heat Conduction with Engineering, Geological, and Other Applications[J]. Journal of Geology, 2009, 63(63):196-196.
- Kavanaugh S P. Simulation and experimental verification of vertical ground-coupled heat pump systems[J]. International Journal of Energy Research, 1985, 21(8):707-722.
- Kaltreider C, Krarti M, McCartney J. Heat transfer analysis of thermo-active foundations[J]. Energy & Buildings, 2015, 86:492-501.
- Lee C K, Lam H N. Computer simulation of borehole ground heat exchangers for geothermal heat pump systems[J]. Renewable Energy, 2008, 33(6):1286-1296.
- Lund J W, Freeston D H, Boyd T L. Direct utilization of geothermal energy 2010 worldwide review[J]. Energies, 2010, 3(8):1443-1471.
- Lyu Z, Song X, Li G, et al. Numerical Analysis of Characteristics of a Single U-tube Downhole Heat Exchanger in the Borehole for Geothermal Wells[J]. Energy, 2017, 125:186-196.
- Nasruddin, Alhamid M I, Daud Y, et al. Potential of geothermal energy for electricity generation in Indonesia: A review[J]. Renewable & Sustainable Energy Reviews, 2016, 53:733-740.
- Rees S J. An extended two-dimensional borehole heat exchanger model for simulation of short and medium timescale thermal response[J]. Renewable Energy, 2015, 83:518-526.
- Rees S J, He M. A three-dimensional numerical model of borehole heat exchanger heat transfer and fluid flow[J]. Geothermics, 2013, 46(4):1-13.

- Starace G, Congedo P, Colangelo G. Horizontal Heat Exchangers for GSHP. Efficiency and Cost Investigation for Three Different Applications[C]// Ecos2005- International Conference on Efficiency, Cost, Optimization, Simulation and Environment. 2005.
- Takemitsu N. An analytical study of the standard k-epsilon model[J]. *Journal of Fluids Engineering*, 1990, 112(6):192-198.
- Wagner W, Pruß A. The IAPWS Formulation 1995 for the Thermodynamic Properties of Ordinary Water Substance for General and Scientific Use[J]. *Journal of Physical & Chemical Reference Data*, 2002, 31(2):387-535.
- Xie G, Sunden B, Wang Q, et al. Performance predictions of laminar and turbulent heat transfer and fluid flow of heat exchangers having large tube-diameter and large tube-row by artificial neural networks[J]. *International Journal of Heat & Mass Transfer*, 2009, 52(11–12):2484-2497.
- Yavuzturk C, Spitler J D, Rees S J. A transient two-dimensional finite volume model for the simulation of vertical U-tube ground heat exchangers[J]. 1999.
- Zeng H, Diao N, Fang Z. Heat transfer analysis of boreholes in vertical ground heat exchangers[J]. *International Journal of Heat & Mass Transfer*, 2003, 46(23):4467-4481.
- Zeng H Y, Diao N R, Fang Z H. A finite line-source model for boreholes in geothermal heat exchangers[J]. *Heat Transfer-Asian Research*, 2002, 31(7):558-567.
- Zhongjian Li, Maoyu Zheng. Development of a numerical model for the simulation of vertical U-tube ground heat exchangers[J]. *Applied Thermal Engineering*, 2009, 29(5):920-924.